JOURNAL OF GUIDANCE, CONTROL, AND DYNAMICS
Vol. 19, No. 5, September–October 1996

Momentum Transfer in Two-Rotor Gyrostats

Christopher D. Hall*
U.S. Air Force Institute of Technology, Wright–Patterson Air Force Base, Ohio 45433

The orientation of a spacecraft can be changed efficiently by transferring angular momentum between the platform and internal momentum wheels using internal torques. The speed of such maneuvers depends on the size of the internal torques and may be limited by the effects of excitation of any flexible elements of the spacecraft. The internal torques required to accomplish such maneuvers arise in various forms. Three types of torque are considered: constant torques for a simple momentum transfer, viscous torques attributable to bearing friction, and time-varying torques defined by a suitable control law. A previously developed graphic result for single-rotor gyrostats is extended to the multiple-rotor case and used to illustrate the different trajectories for the two-rotor gyrostat. A novel feature is the development of stationary-platform rotational maneuvers in which the platform's angular velocity is small throughout the maneuver. These maneuvers are based on a simple control law and are not restricted to small angles.

Introduction

IT is possible to reorient a torque-free rigid body by transferring angular momentum between the body and internal momentum wheels or rotors using internal torques. If the rotors are axisymmetric and constrained to relative rotation about their symmetry axes, then the system is called a gyrostat, and as described below, some analytical results are available. If the rotors are asymmetric, unbalanced, or both, then resonances may occur that increase the likelihood of failure of a momentum transfer maneuver, especially if the internal torques are small. These failures have been studied by numerous researchers.[1]

Several aspects of momentum transfer in two-rotor gyrostats are studied here. We consider three specific cases: both rotors torqued by constant-torque motors; one rotor torqued by a constant-torque motor with the other experiencing only a viscous damping torque; and both rotors subject to time-varying torques based on a simple control law. The time-varying torque control law is based on a novel approach that leads to stationary-platform maneuvers. The control law makes possible large-angle rotational maneuvers in which the angular velocity of the body remains small throughout the maneuver.

Momentum-transfer approaches involving gyrostat models have been developed by many researchers. Anchev[2] derived a control law for maneuvering a three-rotor gyrostat from the gravity-gradient equilibrium orientation to one of the orbiting gyrostat equilibria. Barba and Aubrun[3] used an energy approach to describe the spinup maneuver for an axial gyrostat with constant internal torque. Hubert[4,5] extended their work with the addition of energy dissipation by a viscously damped rotor. Vigneron and Staley[6] designed a switching control strategy to minimize the final nutation angle. Hall and Rand[7] reduced the spinup problem for axial gyrostats to the study of a single first-order equation. Hall extended this to include arbitrary rotor alignment[8] and later to include multiple rotors.[9] Hall[9] also includes a survey of the literature on momentum transfer. Krishnan et al.[10] studied the control of a zero-momentum two-rotor gyrostat.

A large body of work on the optimal control of momentum transfer has been contributed by Junkins and colleagues. Much of this work is combined in a consistent notation in the monograph by Junkins and Turner.[11] In particular, they compare Barba and Aubrun's maneuver[3] with an optimal control solution that minimizes the final angular velocity of the platform and the total control torque.[11] The two solutions are similar, but the Barba and Aubrun approach has the advantage of simplicity because the torque is constant. Thus the constant-torque maneuver provides a nearly optimal solution to the given momentum transfer problem for axial gyrostats. Note that the success of this maneuver depends on the use of a small torque; thus the maneuver is not time-optimal. For multiple-rotor gyrostats, constant-torque maneuvers may be nearly optimal for some situations, but are decidedly not for others. The stationary-platform maneuvers developed here provide nearly optimal solutions to the problem of slowly reorienting a multiple-rotor gyrostat from one orientation to another while simultaneously minimizing the platform angular velocity and the control effort.

Presented as AAS Paper 95-205 at the AAS/AIAA Space Flight Mechanics Conference, Albuquerque, NM, Feb. 13–16, 1995; received May 5, 1995; revision received April 10, 1996; accepted for publication April 10, 1996.

*Assistant Professor of Aerospace and Systems Engineering. Senior Member AIAA.

Equations of Motion

Although we are interested in two-rotor gyrostats here, no complexity is added by first developing the equations of motion for an N-rotor gyrostat. Hence, we begin with the equations of motion for a gyrostat consisting of a rigid platform with N axisymmetric rotors. Internal torques are available to change the angular momentum of the rotors, which in general results in a change in orientation and angular velocity of the platform. As in previous work,[8,9] we use dimensionless variables. The N-rotor gyrostat model is depicted in Fig. 1, where $\mathcal{P}$ denotes the asymmetric platform and $\mathcal{R}_j$ denotes the jth rotor, which is constrained to rotate relative to $\mathcal{P}$ about the rotor symmetry axis $\boldsymbol{a}_j$. The gyrostat is denoted by $\mathcal{P}+\mathcal{R}$. Referring to Fig. 1, we define the following symbols:

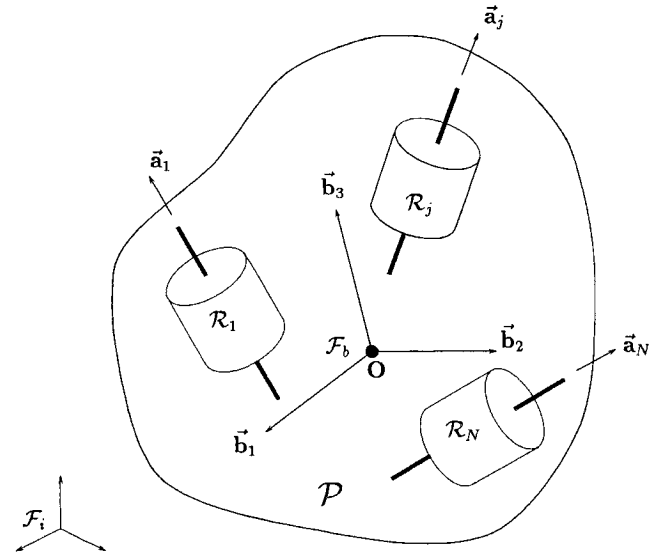

Fig. 1 *N*-rotor gyrostat model.

$\boldsymbol{a}_j$ = axis of relative rotation of $\mathcal{R}_j$, fixed in $\mathcal{F}_b$, $j = 1, \ldots, N$
$\boldsymbol{b}_i$ = orthonormal basis for $\mathcal{F}_b$, $i = 1, 2, 3$
$\mathcal{F}_b$ = reference frame fixed in $\mathcal{P}$
$\mathcal{F}_i$ = inertial reference frame
$\boldsymbol{I}$ = moment of inertia tensor of $\mathcal{P} + \mathcal{R}$ about $\boldsymbol{O}$
$\boldsymbol{I}_s$ = diagonal $N \times N$ matrix of axial moments of inertia of rotors
$\boldsymbol{O}$ = mass center of $\mathcal{P} + \mathcal{R}$ and origin of $\mathcal{F}_b$
$\boldsymbol{\omega}$ = angular velocity of $\mathcal{F}_b$ relative to $\mathcal{F}_i$
$\boldsymbol{\omega}_s$ = $N \times 1$ matrix of rotor angular velocities relative to $\mathcal{F}_b$

All variables and parameters are dimensionless.[8,9] All vectors and tensors are expressed in a platform-fixed nonprincipal frame $\mathcal{F}_b$, and the axial vectors $\boldsymbol{a}_j$ are collected as columns of a $3 \times N$ matrix $\boldsymbol{A} = [\boldsymbol{a}_1 \cdots \boldsymbol{a}_N]$. The nonprincipal frame is chosen so that the matrix $\boldsymbol{J} = \boldsymbol{I} - \boldsymbol{A}\boldsymbol{I}_s\boldsymbol{A}^T$ is diagonal. The dimensionless angular velocity of the platform may be expressed as

$$\boldsymbol{\omega} = \boldsymbol{J}^{-1}(\boldsymbol{x} - \boldsymbol{A}\boldsymbol{\mu}) \tag{1}$$

where $\boldsymbol{x}$ is the angular momentum vector and $\boldsymbol{\mu}$ is the $N \times 1$ vector of rotor momenta relative to inertial space. The torque-free kinetic equations of motion for this system may be put into a dimensionless, noncanonical Hamiltonian form as

$$\dot{\boldsymbol{x}} = \boldsymbol{x}^{\times} \nabla H \tag{2}$$

$$\dot{\boldsymbol{\mu}} = \boldsymbol{\varepsilon} \tag{3}$$

where H is the Hamiltonian and $\boldsymbol{\varepsilon}$ is the $N \times 1$ vector of torques applied to the rotors by the platform. The angular-momentum vector is normalized to unit length, based on conservation of angular momentum, which is expressed as

$$C = \boldsymbol{x}^T\boldsymbol{x}/2 = \tfrac{1}{2} \tag{4}$$

The ∇ operator is with respect to the dimensionless angular momentum $\boldsymbol{x}$, and the Hamiltonian H is

$$H = \tfrac{1}{2}\boldsymbol{x}^T\boldsymbol{J}^{-1}\boldsymbol{x} - \boldsymbol{\mu}^T\boldsymbol{A}^T\boldsymbol{J}^{-1}\boldsymbol{x} + f(C) \tag{5}$$

which satisfies

$$\dot{H} = \boldsymbol{\varepsilon}^T\frac{\partial H}{\partial \boldsymbol{\mu}} = -\boldsymbol{\varepsilon}^T\boldsymbol{A}^T\boldsymbol{J}^{-1}\boldsymbol{x} \tag{6}$$

Note that the $f(C)$ in the definition of the Hamiltonian represents an arbitrary function of C, which may be used to simplify the Hamiltonian. As shown elsewhere,[8] the fact that ∇C lies in the null space of $\boldsymbol{x}^{\times}$ implies that addition of this term has no effect on the equations of motion.

Equation (2) is a noncanonical Hamiltonian system. If $\boldsymbol{\varepsilon} = 0$, it is both autonomous and integrable. If $\boldsymbol{\varepsilon} = \text{const} \neq 0$, Eq. (3) is directly integrable, and Eq. (2) is nonautonomous because H depends on $\boldsymbol{\mu}$. In this case, the method of averaging can be used to reduce the equations of motion to a single first-order differential equation.[7–9] In other cases of interest, some of the torques may be constant, some may depend on the gyrostat angular momenta through a suitable feedback control law, and others may depend on the relative rotor momenta attributable to viscous damping.

If one or more viscously damped rotors are used to provide energy dissipation, then a damped rotor, say $\mathcal{R}_j$, normally will come to rest eventually relative to the platform; i.e., that rotor's relative angular velocity ω_{sj} tends to 0 as $t \to \infty$. The damping torque for a viscously damped rotor is easily shown to be

$$\varepsilon_j = -\gamma_j\left[\mu_j - I_{sj}\boldsymbol{a}_j^T\boldsymbol{J}^{-1}(\boldsymbol{x} - \boldsymbol{A}\boldsymbol{\mu})\right] \tag{7}$$

where $\gamma_j > 0$ is a dimensionless damping coefficient and the term in brackets is the angular momentum of $\mathcal{R}_j$ relative to $\mathcal{P}$, $I_{sj}\omega_{sj}$.

The all-spun condition, also called the locked-rotor condition because all of the rotors are at rest relative to the platform, is defined by $\boldsymbol{\omega}_s = 0$, which leads to

$$\boldsymbol{\mu}_{as} = \boldsymbol{I}_s\boldsymbol{A}^T\boldsymbol{I}^{-1}\boldsymbol{x} \tag{8}$$

This corresponds to a rigid body with inertia $\boldsymbol{I}$ and is the starting condition for an initial attitude acquisition maneuver. To compute $\boldsymbol{\mu}_{as}$ for steady spins, we use the principal frame of the gyrostat, because $\boldsymbol{I}$ is diagonal, and the rigid body equilibria are simply steady spins about the principal axes.

Another useful state is the stationary-platform condition, wherein the platform is fixed in inertial space and all the angular momentum is in the rotors. This condition is defined by $\boldsymbol{\omega} = 0$, which, from Eq. (1), leads to

$$\boldsymbol{x}_{sp} = \boldsymbol{A}\boldsymbol{\mu} \tag{9}$$

Not all values of $\boldsymbol{\mu}$ admit a stationary platform, however. Because conservation of angular momentum requires $\boldsymbol{x}^T\boldsymbol{x} = 1$, a necessary condition for a stationary platform is that the rotor momenta satisfy

$$\boldsymbol{\mu}_{sp}^T\boldsymbol{A}^T\boldsymbol{A}\boldsymbol{\mu}_{sp} = 1 \tag{10}$$

The quadratic form on the left-hand side of Eq. (10) is positive definite, so that Eq. (10) defines an ellipsoid in the N-dimensional $\boldsymbol{\mu}$ space. This condition is used below to develop stationary-platform rotational maneuvers. For given $\boldsymbol{\mu}$ satisfying Eq. (10), the stationary-platform system angular momentum is uniquely determined by Eq. (9). However, the gyrostat attitude is only determined to within a rotation about the angular-momentum vector.

Although the results in the remainder of the paper are relevant to N-rotor gyrostats, we illustrate the basic ideas using a specific gyrostat with $N = 2$. The dimensionless parameters of the two-rotor gyrostat used for the numerical calculations are as follows: The principal moments of inertia are $(100, 70, 40)/210$. The rotor axial moments of inertia are $I_{s1} = 15/210$ and $I_{s2} = 5/210$. (The divisor 210 is the characteristic moment of inertia tr $\tilde{\boldsymbol{I}}$ used in the nondimensionalization.[8]) The rotor axis vectors in the principal frame are $\boldsymbol{a}_1 = \sqrt{3}(1, 1, 1)/3$ and $\boldsymbol{a}_2 = (-1, -2, 2)/3$. The rotation matrix that diagonalizes $\boldsymbol{J} = \boldsymbol{I} - \boldsymbol{A}\boldsymbol{I}_s\boldsymbol{A}^T$ is

$$\boldsymbol{Q} = \begin{bmatrix} 0.9827 & 0.1707 & 0.0722 \\ -0.1776 & 0.9785 & 0.1045 \\ -0.0528 & -0.1156 & 0.9915 \end{bmatrix} \tag{11}$$

The diagonal elements of $\boldsymbol{J}$ in this frame are (0.4560, 0.2954, 0.1533). The rotor axis vectors in the nonprincipal frame are $\boldsymbol{a}_1 = (0.4343, 0.5968, 0.1905)$ and $\boldsymbol{a}_2 = (-0.2444, -0.7863, 0.5675)$. For computing H, we use $f(C) = -C/J_1$.

Slow State Space

In the case where $\boldsymbol{\varepsilon} = 0$, the equations of motion are integrable. Furthermore, there are either two, four, or six steady spins, depending on the values of the rotor momenta $\boldsymbol{\mu}$. Each steady spin has associated with it the values of the components of $\boldsymbol{\mu}$ and the value of the Hamiltonian, and these can be used to construct a bifurcation diagram in $\boldsymbol{\mu}H$ space. The $\boldsymbol{\mu}H$ bifurcation diagram for the example two-rotor gyrostat is shown in Fig. 2. The surfaces shown in this figure are restricted to $\mu_2 > 0$, $\mu_1^2 + \mu_2^2 < 0.4$ for clarity. Some of the surfaces extend to infinity in the μ_1 and μ_2 directions. Calculation of the surfaces uses Euler–Newton continuation[12] as described elsewhere.[8,9]

The surfaces are identified by the $\boldsymbol{\mu} = 0$ equilibria from which they emanate. For $\boldsymbol{\mu} = 0$, the gyrostat is equivalent to a simple rigid body with inertia matrix $\boldsymbol{J}$, and the equilibrium motions are steady spins about the principal axes of this fictitious body. We

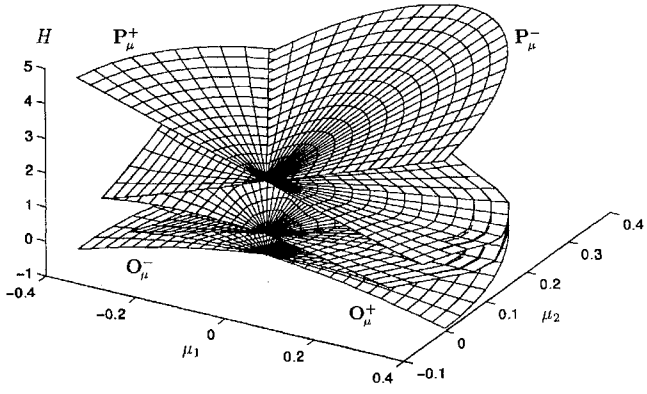

Fig. 2 $\mu_1\mu_2H$ relative equilibrium surfaces.

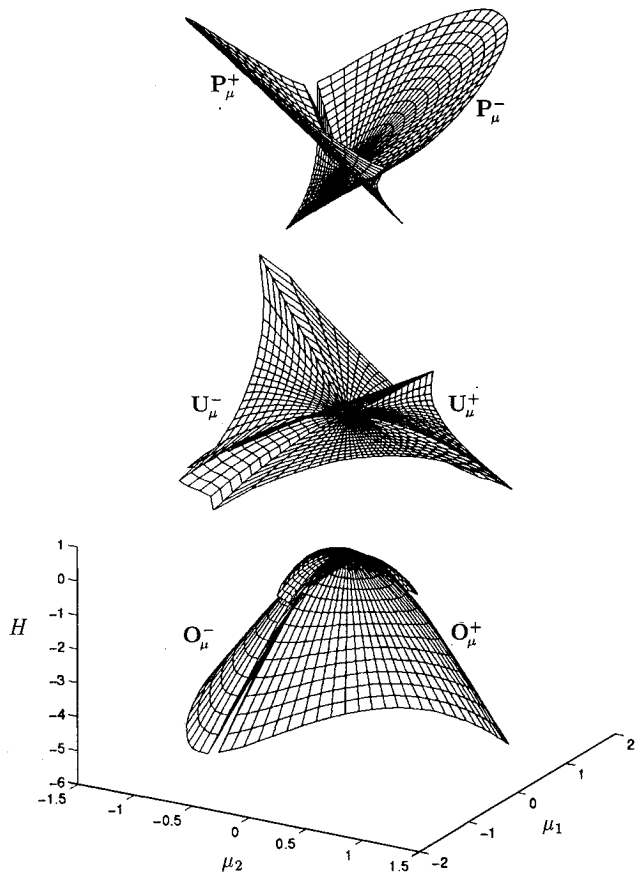

Fig. 3 Exploded view of the three pairs of equilibrium surfaces.

assume without loss of generality that $J_1 > J_2 > J_3$, in which case $\boldsymbol{x} = (\pm 1, 0, 0)$ correspond to stable steady spins about the major or oblate axis. Similarly, $\boldsymbol{x} = (0, 0, \pm 1)$ correspond to stable steady spins about the minor or prolate axis and $\boldsymbol{x} = (0, \pm 1, 0)$ correspond to unstable steady spins about the intermediate axis. The symbols $\mathbf{O}_\mu^\pm$, $\mathbf{U}_\mu^\pm$, and $\mathbf{P}_\mu^\pm$ are used to denote oblate, unstable, and prolate. The superscripts $\pm$ identify which of the two possible $\boldsymbol{\mu} = 0$ equilibria the surface emanates from, and the subscript μ denotes that the equilibrium depends on the specific values of μ. For example, the $\mathbf{O}_\mu^+$ surface includes the $\boldsymbol{\mu} = 0$ equilibrium corresponding to a steady spin about the $\hat{\boldsymbol{b}}_1$ axis. The three pairs of surfaces are shown in an exploded view in Fig. 3. The surfaces can be identified with the equilibria as shown on momentum spheres.[13]

The equilibrium surfaces are useful in a number of ways. As in the single-rotor case, the surfaces in the μH space constitute a bifurcation diagram, illustrating the changing number of equilibria as the rotor momenta $\boldsymbol{\mu}$ are varied. In the undamped, unperturbed system ($\boldsymbol{\varepsilon} = 0$), the $\mathbf{O}_\mu^\pm$ and $\mathbf{P}_\mu^\pm$ surfaces correspond to stable equilibria (centers) and the $\mathbf{U}_\mu^\pm$ surfaces correspond to unstable equilibria (saddles). The cusplike structures in Fig. 2 correspond to turning points in the full phase space of the system, where saddles and centers coalesce and disappear. In the presence of damping, but with no motor torque [$\varepsilon_1 = 0$, ε_2 defined by Eq. (7)], equilibria in the $\mathbf{O}_\mu^\pm$ surfaces become asymptotically stable, and the $\mathbf{P}_\mu^\pm$ surfaces become unstable, similar to the rigid body with energy dissipation. This is entirely analogous to the well-known major-axis rule for quasirigid bodies.[13]

In the case where the motor torques are all small constants, it can be shown using averaging[7–9] that the μH space is an approximate slow state space for the system. The surfaces of equilibria contain exact solutions to the averaged equations, and initial conditions in this space lead approximately to unique trajectories in the slow space, as long as no resonance zones are traversed. The resonance zones correspond to the separatrices of the $\boldsymbol{\varepsilon} = 0$ system, and thus to the $\mathbf{U}_\mu^\pm$ equilibrium surfaces.

Thus, with small constant motor torques, any trajectory beginning near a stable equilibrium surface will remain near the surface unless one of the turning points is encountered. Such an encounter is called an instantaneous separatrix crossing or passage through resonance and typically results in a large amplitude motion of the platform. This is strictly valid only for small constant torques but gives qualitatively correct results for torques that vary slowly with time as well.

If ε_1 is a small constant, ε_2 is a viscous damping torque given by Eq. (7), and the initial condition is near an asymptotically stable equilibrium ($\mathbf{O}_\mu^\pm$), then the trajectory also will remain near the surface. Again, it is possible that a separatrix crossing will lead to large oscillations, but the damping will lead to an asymptotically stable equilibrium surface.

A final case of interest is based on the stationary-platform condition, $\boldsymbol{x} = \boldsymbol{A}\boldsymbol{\mu}$, where the gyrostat is in equilibrium and the platform is not rotating ($\boldsymbol{\omega} = 0$). Because $\boldsymbol{x}^T\boldsymbol{x} = 1$, this gives a quadratic-form condition [Eqs. (9) and (10)] on $\boldsymbol{\mu}$ leading to a connected set of equilibria corresponding to a motionless platform. If the torques $\boldsymbol{\varepsilon}$ are chosen so that the rotor momenta $\boldsymbol{\mu}$ remain in this set, then the gyrostat can be reoriented through large angle maneuvers while maintaining small oscillations of the platform. Note that this does not completely address the reorientation problem, because the precession about the angular-momentum vector is not determined.

Momentum-Transfer Dynamics

In this section, we present numerically computed momentum-transfer trajectories for the example two-rotor gyrostat, using the equilibrium surfaces in $\mu_1\mu_2 H$ space as a framework to discuss the trajectories. Three specific cases are considered: constant torques, one constant torque with the other attributable to viscous damping, and controlled torques for stationary-platform maneuvers.

Constant Torques

Constant motor torques might be used in an initial attitude acquisition maneuver, where the angular momentum is transferred from the platform to the rotors. The Barba and Aubrun[3] maneuver, for example, is a nearly optimal constant torque maneuver for a single-rotor axial gyrostat. In the example used here, the rotors are initially in the all-spun condition, defined by Eq. (8). Four of the all-spun equilibria are the major and minor axis spins, which are all reasonable initial conditions for a momentum-transfer trajectory. The other two are intermediate axis spins that would require external torques for stabilization and hence are not of interest here.

One trajectory is shown in Fig. 4, beginning at the stable all-spun equilibrium on the $\mathbf{O}_\mu^+$ surface. The spinup torques are $\boldsymbol{\varepsilon} = (0.01, 0.01)$. Note that the trajectory remains near the $\mathbf{O}_\mu^+$ equilibrium surface. The trajectory for the $\mathbf{O}_\mu^-$ all-spun equilibrium is shown in Fig. 5. Note that the surface ends (in a bifurcation) before the trajectory does. Thus this trajectory is no longer near an equilibrium surface. The departure is associated with the instantaneous separatrix crossing. To illustrate the significance of the difference between the two types of trajectories, in Fig. 6 the $\hat{\boldsymbol{b}}_1$ components of the angular velocity for the two trajectories are compared. The $\mathbf{O}_\mu^-$ trajectory oscillates with much larger amplitude because of the separatrix crossing. A simple scheme has been suggested for avoiding this resonance zone.[14]

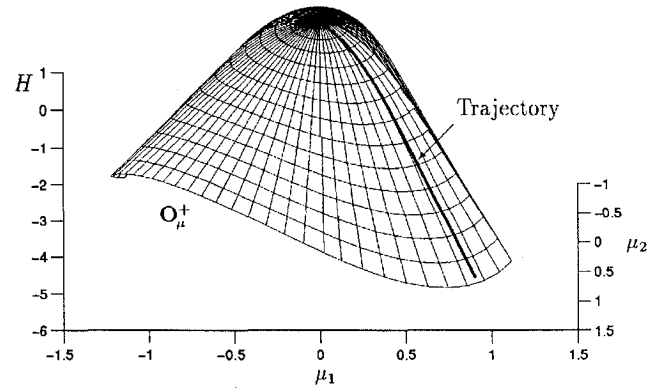

Fig. 4 $\mathbf{O}_\mu^+$ equilibrium surface with constant-torque trajectory beginning at all-spun condition.

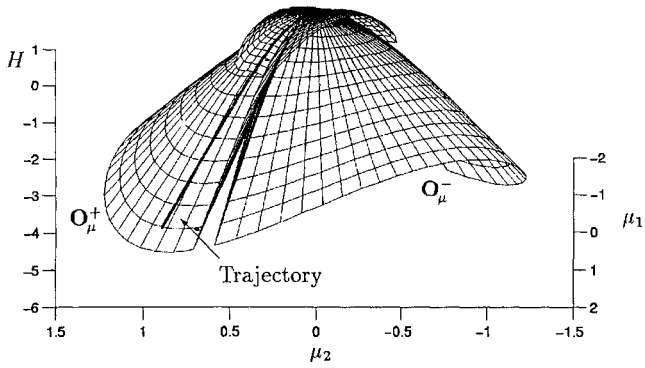

Fig. 5 $O_\mu^\pm$ equilibrium surfaces with constant-torque trajectory beginning at O_μ^- all-spun condition.

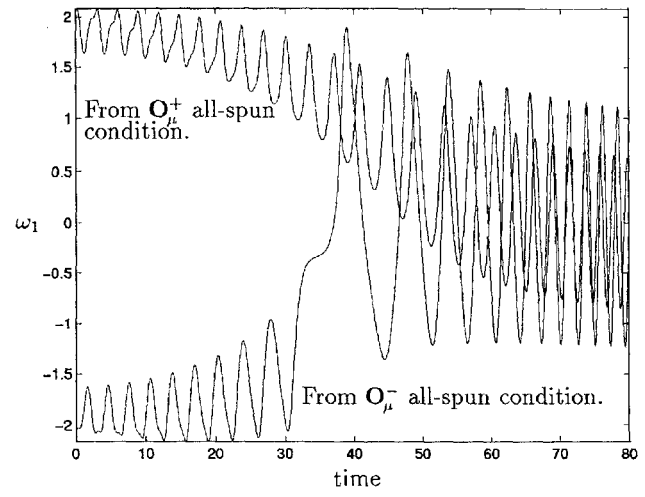

Fig. 6 Comparison of ω_1 for the trajectories in the previous two plots.

Constant Torque and Viscous Damping Torque

This case is relevant for a number of applications. A viscously damped rotor could actually be used to provide the energy dissipation onboard a spacecraft with momentum wheels, the damped rotor could be a simple model of a ring damper filled with viscous fluid, or a failed motor could result in a damped momentum wheel. Hubert[5] used a viscously damped rotor to model the energy dissipation in a dual-spin spacecraft. The limiting case where the damped rotor's axial inertia goes to zero could be used to provide analytical results for the energy-sink hypothesis.

Here we illustrate the effects of the damped rotor by showing trajectories in the slow state space. It is possible to show that some equilibria on the $\mathbf{O}_\mu^\pm$ equilibrium surfaces in the μH space become asymptotically stable in the presence of energy dissipation, whereas the $\mathbf{P}_\mu^\pm$ surfaces become unstable. More precisely, for a fixed constant value of μ_1, the all-spun condition for $\mathcal{R}_2$ determines an asymptotically stable equilibrium on at least one of the two $\mathbf{O}_\mu^\pm$ surfaces. For example, if $\mu_1 = 1$, then $\boldsymbol{x} = \boldsymbol{a}_1$, $\mu_2 = 0$, is an asymptotically stable equilibrium for $\varepsilon_1 = 0$, as may be shown by checking the eigenvalues of the linearized system.

In Fig. 7, we show two trajectories beginning at the $\mathbf{P}_\mu^-$ all-spun initial condition. For both trajectories, $\varepsilon_1 = 0.01$. For one of the trajectories, only $\mathcal{R}_1$ experiences an axial torque; i.e., $\varepsilon_2 = 0$. For the other trajectory, $\mathcal{R}_2$ experiences an axial torque attributable to viscous damping, with $\gamma_2 = 1$, as defined by Eq. (7). Referring to the figure, it is easy to see that the stability of the $\mathbf{P}_\mu^-$ surface in the undamped case is destroyed by the addition of energy dissipation. The trajectory with damping is attracted to the $\mathbf{O}_\mu^+$ surface, which is asymptotically stable in the presence of damping.

Stationary-Platform Maneuver Torques

In this section, we develop and demonstrate the concept of stationary-platform maneuvers. By combining the μH description of momentum transfer with the stationary-platform conditions in Eqs. (9) and (10), we obtain a simple control law based on the following idea: If the torques are small, but not necessarily constant, then it is reasonable to suppose that the qualitative results obtained by averaging will remain valid. Under this hypothesis, trajectories that start on or near a stable equilibrium surface in μH space will remain near the equilibrium surface as long as no resonance zone (instantaneous separatrix) is traversed. If the initial condition is also near a stationary-platform equilibrium ($\omega = 0$) and the torques are chosen so that the trajectory in μ space satisfies the stationary-platform condition ($\mu^T A^T A \mu = 1$), then the angular velocity of the platform will remain small throughout the maneuver. The advantage of such a trajectory is that the small platform angular velocities are less likely to excite vibrations in flexible components. Of course, the platform is not actually stationary during the maneuver. The term is used to indicate that the motion remains near a stationary-platform equilibrium of the $\varepsilon = 0$ system.

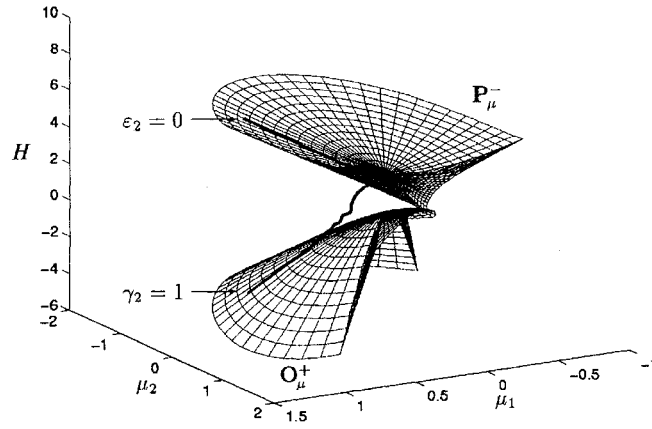

Fig. 7 $\mathbf{P}_\mu^-$ and $\mathbf{O}_\mu^+$ equilibrium surfaces, with trajectories starting at $\mathbf{P}_\mu^-$ all-spun condition.

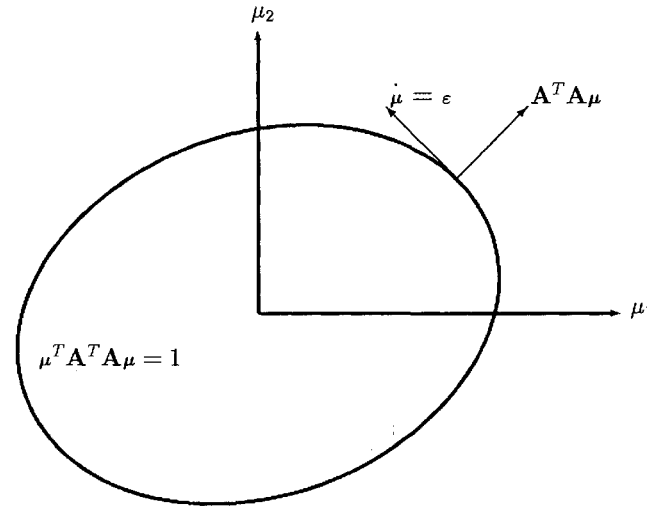

Fig. 8 Stationary-platform ellipse in $\mu_1\mu_2$ plane.

For stationary-platform maneuvers, we assume initial conditions on $\boldsymbol{x}$ and μ that satisfy Eqs. (9) and (10); i.e., $\boldsymbol{x} = \boldsymbol{A}\mu$ and $\mu^T \boldsymbol{A}^T \boldsymbol{A} \mu = 1$. (Note that for $N \geq 3$, and rank $\boldsymbol{A} = 3$, any platform orientation is possible.) Then the spinup torques ε are chosen such that the condition on μ is satisfied throughout the maneuver. Differentiation of Eq. (10) with respect to time shows that any ε that is orthogonal to $\boldsymbol{A}^T \boldsymbol{A} \mu$ will yield such a maneuver. As noted earlier, Eq. (10) defines an ellipsoid in the N-dimensional μ space, which can be thought of as an elliptic cylinder in the $(N+1)$-dimensional μH space. Thus the torque vector ε must lie in the tangent space of the ellipsoid. For the $N = 2$ case, the ellipsoid is a simple ellipse, and the trajectory in μ space simply traces the ellipse, as illustrated in Fig. 8.

The intersection of the elliptic cylinder with the equilibrium surfaces in μH space includes the set of all possible stationary-platform equilibria; however, because Eq. (9) also must be satisfied, the intersection includes equilibria for which the platform is not stationary. The set of stationary-platform equilibria is in the $\mathbf{O}_\mu^\pm$ surfaces

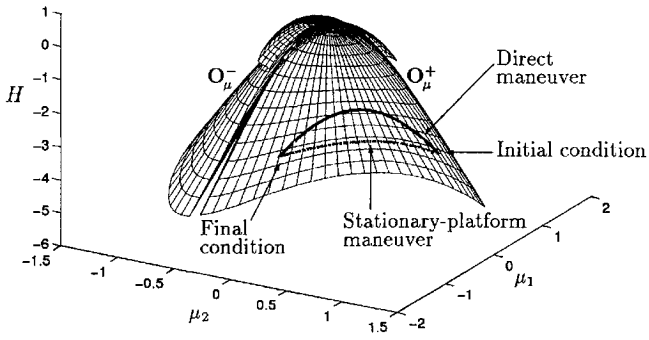

Fig. 9 Stationary-platform trajectory compared with direct momentum transfer on the O_μ^+ surface.

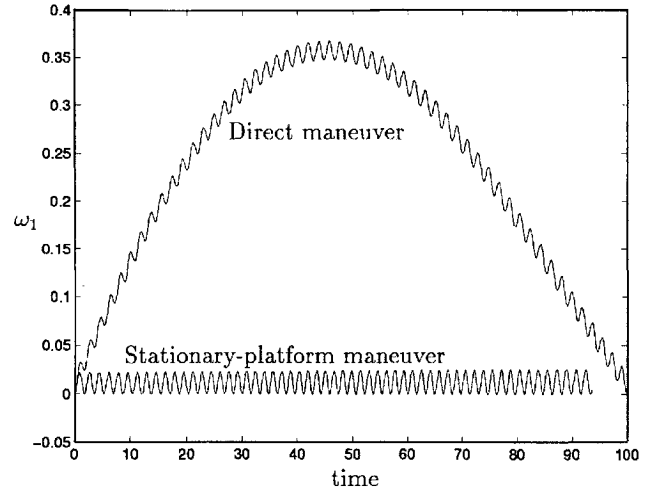

Fig. 10 Comparison of ω_1 for the two trajectories in the preceding plot.

exclusively. For the two-rotor case, it is straightforward to verify that the set of stationary-platform equilibria is the intersection of the elliptic cylinder $\mu_1^2 + 2\boldsymbol{a}_1^T\boldsymbol{a}_2\mu_1\mu_2 + \mu_2^2 = 1$ and the $\mathbf{O}_\mu^\pm$ surfaces.

For the example here, we choose initial and final conditions where all of the angular momentum is in one of the rotors: Initially, $\mathcal{R}_1$ contains all of the angular momentum, and at the end of the maneuver, the momentum has been transferred to $\mathcal{R}_2$. Thus we begin with $\boldsymbol{\mu} = (1, 0)$ and $\boldsymbol{x} = \boldsymbol{a}_1$, and the desired final conditions are $\boldsymbol{\mu} = (0, -1)$ and $\boldsymbol{x} = -\boldsymbol{a}_2$. This amounts to a slightly greater than 100-deg rotational maneuver.

This maneuver could be accomplished with constant spinup torques; i.e., a reasonable choice for the spinup torques would be $\boldsymbol{\varepsilon} = \epsilon(-1, -1)$, where ϵ is a small positive constant ($\epsilon = 0.01$ in the example). This set of spinup torques gives a straight-line trajectory in the $\mu_1\mu_2$ plane, corresponding to the curved trajectory on (actually just close to) the $\mathbf{O}_\mu^+$ surface, as shown in Fig. 9. No separatrix crossing occurs, and the averaging results mentioned above are formally valid in this case.

A stationary-platform maneuver for $N = 2$ is obtained with the torque

$$\boldsymbol{\varepsilon} = \epsilon \begin{pmatrix} \boldsymbol{a}_1^T\boldsymbol{a}_2 & 1 \\ -1 & -\boldsymbol{a}_1^T\boldsymbol{a}_2 \end{pmatrix} \boldsymbol{\mu} \tag{12}$$

where ϵ is a small constant that may be positive or negative, depending on which way around the ellipse the trajectory should go. Because $\boldsymbol{\mu}$ lies on the ellipse, it is clear that the torque is bounded, i.e., $\|\boldsymbol{\varepsilon}\| = \mathcal{O}(\epsilon)$. The torque gives an ellipse-segment trajectory in the $\mu_1\mu_2$ plane or the trajectory in the slow state space shown in Fig. 9. The value $\epsilon = 0.015$ was chosen so that the stationary-platform and direct maneuvers take about the same amount of time. The two trajectories are clearly different, as shown in the figure, but the difference, as well as the significance of the stationary-platform approach, is most evident when the angular velocities are plotted vs time, as in Fig. 10, where ω_1 is plotted for the two trajectories. Here it is evident that the stationary-platform trajectory results in a uniformly smaller amplitude of the angular velocity. The other two components of angular velocity behave similarly. Thus the stationary-platform maneuver provides a means of executing a large-angle rotational maneuver while maintaining a small platform angular velocity. If a third, viscously damped, rotor is added, the stationary-platform equilibria become asymptotically stable and the small angular velocity damps out after the maneuver. This is explored in more detail elsewhere.[15]

Note that Eqs. (3) and (12) constitute a constant-coefficient linear system that can be solved in closed form and is decoupled from the platform dynamics. Thus the stationary-platform maneuver is an easy-to-implement open-loop maneuver that is nearly optimal in two ways: the platform angular velocity is small throughout the maneuver, and the motor torque is small throughout the maneuver, because $\|\boldsymbol{\varepsilon}\| = \mathcal{O}(\epsilon)$. Furthermore, because $\boldsymbol{\mu}$ can be expressed in terms of the platform angular velocity $\boldsymbol{\omega}$ and the rotor relative angular velocities $\boldsymbol{\omega}_s$, one could implement the maneuver as a closed-loop control. Questions regarding the stability of a closed-loop stationary-platform maneuver in the presence of uncertainties and disturbances have not been addressed.

Conclusions

The attitude dynamics of momentum transfer in multiple-rotor gyrostats are more easily understood when presented in the context of the slow state space of the rotor momenta and the Hamiltonian. In the two-rotor case, the slow state space is three dimensional, and trajectories can be visualized relative to the equilibrium surfaces. This is useful for identifying the possibility of passage through resonance zones where large oscillations may occur. Previously unreported stationary-platform maneuvers are possible, wherein the angular velocity of the platform remains small throughout the reorientation. These maneuvers are based on a simple, nearly optimal, control law for the momentum-transfer torque, and are not limited to small-angle orientation changes.

References

[1]Tsui, R., and Hall, C. D., "Resonance Capture in Unbalanced Dual-Spin Spacecraft," *Journal of Guidance, Control, and Dynamics*, Vol. 18, No. 6, 1995, pp. 1329–1335.

[2]Anchev, A. A., "Equilibrium Attitude Transitions of a Three-Rotor Gyrostat in a Circular Orbit," *AIAA Journal*, Vol. 11, No. 4, 1973, pp. 467–472.

[3]Barba, P. M., and Aubrun, J. N., "Satellite Attitude Acquisition by Momentum Transfer," *AIAA Journal*, Vol. 14, No. 10, 1976, pp. 1382–1386.

[4]Hubert, C. H., "Dynamics of the Generalized Dual-Spin Turn," *RCA Review*, Vol. 41, No. 3, 1980, pp. 449–471.

[5]Hubert, C. H., "Spacecraft Attitude Acquisition from an Arbitrary Spinning or Tumbled State," *Journal of Guidance and Control*, Vol. 4, No. 2, 1981, pp. 164–170.

[6]Vigneron, F. R., and Staley, D. A., "Satellite Attitude Acquisition by Momentum Transfer—The Controlled Wheel Speed Method," *Celestial Mechanics and Dynamical Astronomy*, Vol. 27, No. 2, 1982, pp. 111–130.

[7]Hall, C. D., and Rand, R. H., "Spinup Dynamics of Axial Dual-Spin Spacecraft," *Journal of Guidance, Control, and Dynamics*, Vol. 17, No. 1, 1994, pp. 30–37.

[8]Hall, C. D., "Spinup Dynamics of Gyrostats," *Journal of Guidance, Control, and Dynamics*, Vol. 18, No. 5, 1995, pp. 1177–1183.

[9]Hall, C. D., "Momentum Transfer in Torque-Free Gyrostats," *Nonlinear Dynamics—The Richard Rand 50th Anniversary Volume*, edited by A. Guran and D. J. Inman, World Scientific, Singapore (to be published).

[10]Krishnan, H., McClamroch, N. H., and Reyhanoglu, M., "Attitude Stabilization of a Rigid Spacecraft Using Two Momentum Wheel Actuators," *Journal of Guidance, Control, and Dynamics*, Vol. 18, No. 2, 1995, pp. 256–263.

[11]Junkins, J. L., and Turner, J. D., *Optimal Spacecraft Rotational Maneuvers*, Elsevier, Amsterdam, 1986, pp. 267–273.

[12]Seydel, R., *From Equilibrium to Chaos: Practical Bifurcation and Stability Analysis*, Elsevier, New York, 1988, Chap. 4.

[13]Hughes, P. C., *Spacecraft Attitude Dynamics*, Wiley, New York, 1986, Chaps. 3, 5, and 6.

[14]Hall, C. D., "Spinup Dynamics of Biaxial Gyrostats," *Journal of the Astronautical Sciences*, Vol. 43, No. 3, 1995, pp. 263–276.

[15]Hall, C. D., "Stationary-Platform Maneuvers of Gyrostat Satellites," *Dynamics and Control of Structures in Space III*, edited by C. L. Kirk and D. J. Inman, Computational Mechanics Publications, Southampton, England, UK, 1996, pp. 337–348.